THE JOURNAL OF BIOLOGICAL CHEMISTRY VOL. 286, NO. 7, pp. 5506–5518, February 18, 2011

Three Phosphatidylglycerol-phosphate Phosphatases in the Inner Membrane of *Escherichia coli*[*S]

Received for publication, October 30, 2010, and in revised form, December 8, 2010 Published, JBC Papers in Press, December 9, 2010, DOI 10.1074/jbc.M110.199265

Yi-Hsueh Lu[1], **Ziqiang Guan, Jinshi Zhao, and Christian R. H. Raetz**[2]

From the Department of Biochemistry, Duke University Medical Center, Durham, North Carolina 27710

The phospholipids of *Escherichia coli* consist mainly of phosphatidylethanolamine, phosphatidylglycerol (PG), and cardiolipin. PG makes up ~25% of the cellular phospholipid and is essential for growth in wild-type cells. PG is synthesized on the inner surface of the inner membrane from cytidine diphosphate-diacylglycerol and glycerol 3-phosphate, generating the precursor phosphatidylglycerol-phosphate (PGP). This compound is present at low levels (~0.1% of the total lipid). Dephosphorylation of PGP to PG is catalyzed by several PGP-phosphatases. The *pgpA* and *pgpB* genes, which encode structurally distinct PGP-phosphatases, were identified previously. Double deletion mutants lacking *pgpA* and *pgpB* are viable and still make PG, suggesting the presence of additional phosphatase(s). We have identified a third PGP-phosphatase gene (previously annotated as *yfhB* but renamed *pgpC*) using an expression cloning strategy. A mutant with deletions in all three phosphatase genes is not viable unless covered by a plasmid expressing either *pgpA*, *pgpB*, or *pgpC*. When the triple mutant is covered with the temperature-sensitive plasmid pMAK705 expressing any one of the three *pgp* genes, the cells grow at 30 but not 42 °C. As growth slows at 42 °C, PGP accumulates to high levels, and the PG content declines. PgpC orthologs are present in many other bacteria.

The phospholipids of *Escherichia coli* are synthesized on the inner leaflet of the inner membrane by a system of enzymes first described by Eugene Kennedy (Fig. 1) (1–6). The process starts with the acylation of glycerol 3-phosphate to generate phosphatidic acid (5), followed by conversion of phosphatidic acid to CDP-diacylglycerol (Fig. 1) (7). This material functions as a donor of phosphatidyl moieties to the primary hydroxyl groups of serine or glycerol 3-phosphate to generate phosphatidylserine or phosphatidylglycerol phosphate (PGP),[3] respectively (Fig. 1) (2, 8). Phosphatidylserine is rapidly decarboxylated to phosphatidylethanolamine (PE), whereas PGP is immediately dephosphorylated to generate phosphatidylglycerol (PG) (Fig. 1) (8, 9). Some of the PG is further converted to cardiolipin (CL) (10). PE, PG, and CL are the major end products of the Kennedy pathway. These substances form the bilayer of the inner membrane and the inner leaflet of the outer membrane (11). The lipid A moiety of lipopolysaccharide covers the outer surface of the outer membrane (12). The levels of the intermediates phosphatidic acid, CDP-diacylglycerol, phosphatidylserine, and PGP are extremely low in wild-type *E. coli*, representing less than 0.2% of the total cellular phospholipid (13–16).

The functions of lipid molecular species are not well understood (4, 6). PG is important for viability in wild-type cells not only because it is a major component of the inner membrane but also because it plays critical roles in the initiation of DNA replication at *oriC* and in SecA-dependent protein translocation (6). However, one can delete the *pgsA* gene (Fig. 1) in *E. coli* cells harboring mutations in the *lpp* gene (17, 18), which encodes the major outer membrane lipoprotein, thereby creating strains that do not produce any PG or CL. How these cells compensate for loss of PG and CL is unclear. They do accumulate some phosphatidic acid, CDP-diacylglycerol, and *N*-acyl-PE, all of which are acidic lipids (18–20).

The conversion of CDP-diacylglycerol to phosphatidylserine or PGP is carried out by the phosphatidyltransferases PssA (21) or PgsA (22), respectively (Fig. 1). These enzymes, as well as the phosphatidylserine decarboxylase (Fig. 1), are encoded by single copy genes, deletions of which result in the expected changes in cellular lipid composition (6). However, the conversion of PGP to PG involves several PGP-phosphatases (16, 23). The PgpA and PgpB phosphatases, encoded by *pgpA* and *pgpB,* respectively, were discovered in 1983 using chemical mutagenesis in conjunction with a colony autoradiography protocol (16, 24). An *E. coli* double mutant with deletions of both genes showed at most ~20-fold of accumulation of PGP (23), raising its concentration from 0.1 to 2.0% of the total lipid (16, 23). Nevertheless, the double deletion mutant grew normally and made wild-type amounts of PG and CL (23). *In vitro* studies showed that residual PGP-phosphatase activity was measurable in the double deletion mutant if the assays were carried out at 30 °C (23). The residual PGP-phosphatase activity present in extracts of the double mutant was inactivated by incubation at 42 °C (23). These findings strongly suggested the existence of one or more additional PGP-phosphatases in *E. coli* (23). However, the missing phosphatase(s) have remained obscure in the 2 decades since the discovery of PgpA and PgpB.

* This work was supported, in whole or in part, by National Institutes of Health Grants GM-51796 (to C. R. H. R.) and the Large Scale Collaborative Grant GM-069338 (to Z. G. and the Lipid MAPS mass spectrometry facility at Duke University).

This paper is dedicated to Professor Eugene P. Kennedy on the occasion of his 91st birthday.

[S] The on-line version of this article (available at http://www.jbc.org) contains supplemental Figs. 1–4, Tables 1 and 2, and additional references.

[1] Present address: The Rockefeller University, New York, NY 10065.

[2] To whom correspondence should be addressed: Dept. of Biochemistry, Duke University Medical Center, P. O. Box 3711, Durham, NC 27710. Tel.: 919-684-3384; Fax: 919-684-8885; E-mail: raetz@biochem.duke.edu.

[3] The abbreviations used are: PGP, phosphatidylglycerol phosphate; CL, cardiolipin; PE, phosphatidylethanolamine; PG, phosphatidylglycerol; ESI, electrospray ionization.

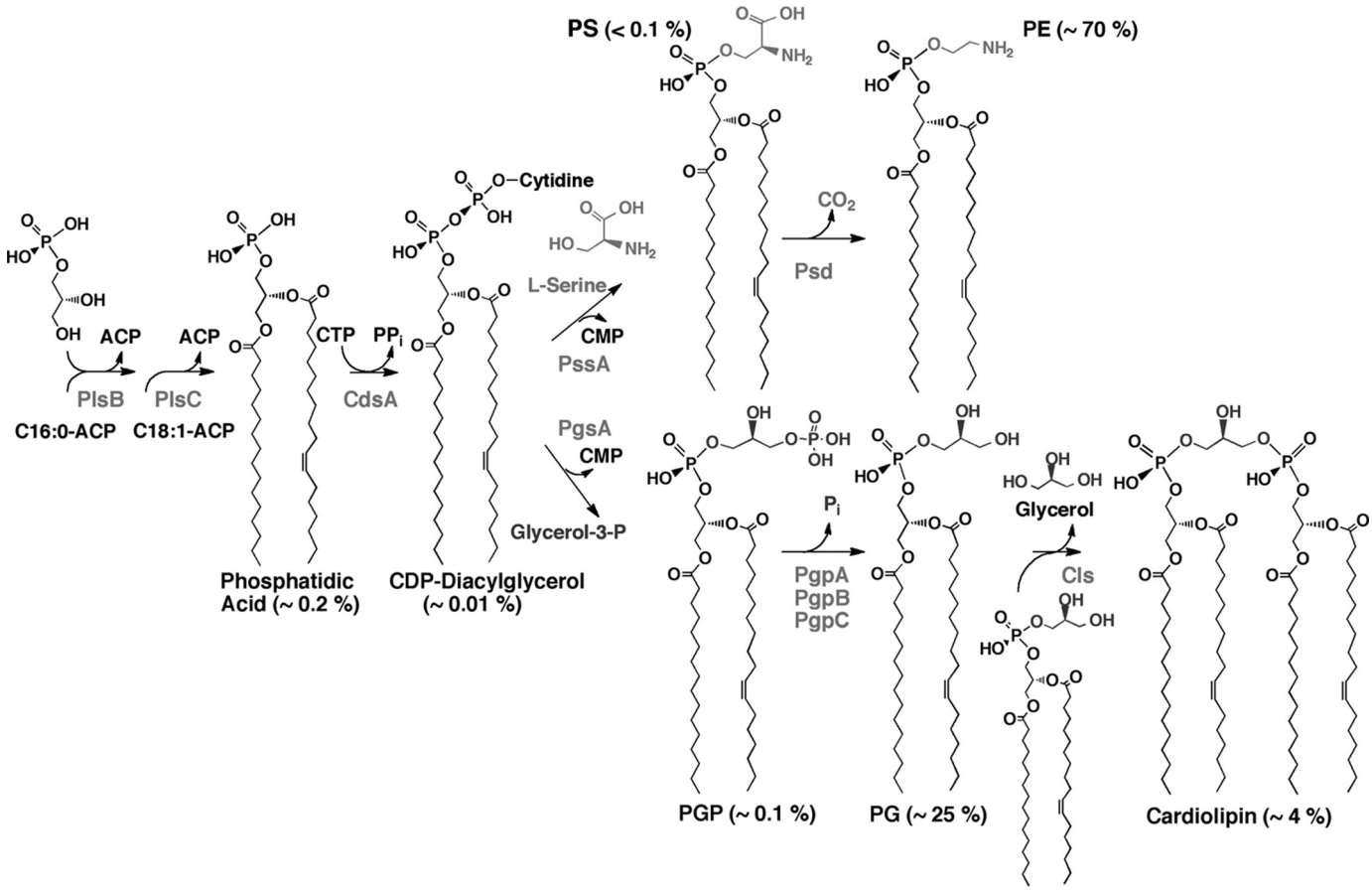

FIGURE 1. **Kennedy pathway for the biosynthesis of *E. coli* phospholipids.** The enzymes responsible for each conversion are named according to their structural genes. In general, a single *E. coli* gene encodes each enzyme. However, the conversion of PGP into PG is catalyzed by three structurally distinct inner membrane phosphatases. PgpA and PgpB were reported previously (16, 23), but double mutants are viable, accumulate only small amounts of PGP, and synthesize normal levels of PG and CL. The PgpC phosphatase, the subject of this study, accounts for the residual PGP-phosphatase activity. The active site of PgpB faces the periplasm (43), whereas those of PgpA and PgpC likely face the cytoplasm. *PS*, phosphatidylserine.

We have now used an expression cloning strategy to identify a third PGP-phosphatase, designated PgpC. An *E. coli* genomic library (25) was transformed into a *pgpApgpB* double deletion mutant, and PGP-phosphatase activity was assayed at room temperature (22 °C) in pooled extracts of 2750 colonies harboring different *E. coli* DNA fragments. The *pgpC* gene (previously annotated as *yfhB*) (26) encodes an inner membrane phosphatase consisting of 211 amino acid residues with a single predicted trans-membrane helix. The *pgpC* gene is essential for growth in a *pgpApgpB* double mutant but not in wild-type cells (27). The triple mutant can be generated when a covering plasmid expressing one of the three PGP-phosphatases is present. If the complemented triple mutant is constructed using the temperature-sensitive replicon pMAK705 (28), the cells lose viability after 3–10 h at 42 °C. Lipid profiling of these strains by mass spectrometry confirmed massive accumulation of PGP at 42 °C, accompanied by the disappearance of PG.

EXPERIMENTAL PROCEDURES

Materials, Reagents, and Growth Conditions—Reagent-grade chloroform, methanol, hydrochloric acid, sulfuric acid, aqueous ammonia, formic acid, pyridine, acetonitrile, isopropyl alcohol, and ethanol were obtained from Sigma. Tryptone and yeast extract were purchased from Difco. Liquid LB medium, which contains 10 g of tryptone, 5 g of yeast extract, and 10 g of NaCl/liter (29), was usually used to grow *E. coli*. Solid medium consisted of LB broth with the addition of 20 g of agar/liter. When necessary, the cultures were supplemented with kanamycin (50 μg/ml), ampicillin (100 μg/ml), or chloramphenicol (25 μg/ml). The pBAD33.1-derived hybrid plasmids (30) were induced with 0.2% L-(+)-arabinose (Sigma), as indicated. Strains were grown at room temperature (22 °C), 30, 37, or 42 °C, as specified; growth, as judged by A_{600}, was monitored with a DU 640 spectrophotometer (Beckman Coulter, Brea, CA).

Bacterial Strains, Plasmids, and General Techniques of DNA Manipulation—All strains and plasmids with their relevant genotypes are listed Tables 1 and 2, respectively. The parental strain *E. coli* W3110 is considered to be wild type with respect to its glycerophospholipid composition. The JW strains were obtained from the single-gene deletion library of *E. coli* K12 known as the Keio collection (27).

PCR amplification of genes from *E. coli* chromosomal DNA was performed in a T3000 Thermocycler (Biometra, Goettingen, Germany), using the KOD Hot Start DNA polymerase (Novagen, Gibbstown, NJ) and following the manufacturer's

protocols. Customized primers were synthesized by Integrated DNA Technology (Coralville, IA). Genomic DNA samples, prepared with the DNeasy kit (Qiagen, Valencia, CA), were used as templates in PCR analysis. When screening for colonies with the correct recombinant gene, colony PCR was performed, followed by DNA sequencing. Gel electrophoresis was performed with 0.7% agarose gels containing SYBR Safe DNA gel stain (Invitrogen). DNA sizes were estimated with the HyperLadder I (Bioline, Taunton, MA) as reference. Gels were viewed with a GelDoc-It Imaging System (UVP, LLC Upland, CA) equipped with a high energy UV lamp. Plasmid extractions employed the QIAprep miniprep kit (Qiagen, Valencia, CA), and other DNA purification procedures employed the QIAquick PCR purification kit and the QIAquick gel extraction kit (Qiagen, Valencia, CA). DNA concentrations were measured directly with a NanoVue Plus spectrophotometer (GE Healthcare). Transformation of plasmid DNA was performed by electroporation, as described previously (31), or by chemical transformation on ice for 30 min, followed by heat shock at 42 °C for 30 s (32). Competent cells for electroporation were prepared as follows; the recipient strain was grown to A_{600} ~0.5. The culture was immediately cooled on ice, and the cells were collected by centrifugation (3500 × *g*) at 4 °C. The cell pellet was washed with cold deionized water four times to remove any remaining electrolytes. If the cells were not used immediately, they were stored at −80 °C as a suspension in 15% glycerol. All gene deletions were confirmed by PCR and DNA sequencing.

Construction of Chromosomal Mutants Lacking the pgp Genes—The *E. coli* K12 single-gene deletion library, known as the Keio collection (27), was employed as the mutation donor to construct a set of isogenic strains lacking one or more of the chromosomal *pgp* genes. The Keio mutant strains each harbor a kanamycin resistance cassette with flanking *FLP* sequences in place of the chromosomal copy of each nonessential gene (27). These kanamycin resistance cassettes can readily be transferred into appropriate recipient strains by $P1_{vir}$ transduction using well established protocols (29). $P1_{vir}$ bacteriophage lysates of strains harboring deletions in *pgpA*, *pgpB*, or *pgpC* were prepared from liquid cultures of Keio strains JW0408, JW1270, and JW5408, respectively. The lysates were used to transduce the desired *pgp* gene deletions into *E. coli* W3110 or its derived strains, as described in Table 1. To construct a mutant with multiple deletions, the kanamycin cassette of the first *pgp* gene that was transferred into W3110 was excised from the chromosome (33, 34), after which the second kanamycin insertion/deletion in a different pgp gene could be introduced by another $P1_{vir}$ transduction. Excision of the kanamycin cassette utilized the plasmid pCP20, the Flp recombinase of which mediates the recombination between the two *FLP* sites and removes the kanamycin cassette, leaving only a scar of one *FLP* sequence on the chromosome (33, 34). The pCP20 transformants were selected for ampicillin resistance at 30 °C, followed by purifying single cells twice at 42 °C in the absence of antibiotic; the 42 °C incubation was necessary for expression of the Flp recombinase and for diluting out the temperature-sensitive replicon pCP20. The desired strain was then obtained by replica plating for ampicillin and kanamycin sensitivity at 30 °C. PCR analysis and DNA sequencing were employed to confirm the genotypes with primers nYL7 to nYL10, nYL33, and nYL34, as explained in supplemental Table 1.

Construction of Plasmids Expressing the pgp Genes—The coding regions of *pgpA, pgpB,* and *pgpC* were amplified by PCR using W3110 genomic DNA as the template and pairs of primers nYL13 and nYL14, nYL15 and nYL16, and nYL29 and nYL30, respectively (supplemental Table 2). The PCR products were purified and subsequently digested with the restriction enzymes NdeI and HindIII in NEB buffer 2 (New England Biolabs, Ipswich, MA) at 37 °C for 2 h. The digested products were purified by gel electrophoresis. Purified plasmid pBAD33.1 (30) was similarly digested, gel-purified, and then treated with calf intestinal alkaline phosphatase in NEB buffer 3 (New England Biolabs, Ipswich, MA) at 37 °C. The vector and the individual digested PCR products were mixed in a 1:3 molar ratio and ligated using T4 DNA ligase in T4 DNA ligase reaction buffer (New England Biolabs, Ipswich, MA) at room temperature for 1 h. The products were transferred into competent cells of *E. coli* DH5α (Invitrogen) by chemical transformation, after which transformants were selected at 37 °C on LB plates containing chloramphenicol. The desired insertions were confirmed by colony PCR and DNA sequencing using the primers nBADfor and nBADrev (supplemental Table 1).

The pMAK705-derived plasmids (Table 2) (28) were constructed using PCR products of the corresponding pBAD33.1-derived hybrid plasmids. Primers nYL35 and nYL36 were designed as follows. nYL35 had an XbaI site before the ribosomal binding site of pBAD33.1, and nYL36 contained a HindIII site for purposes of PCR and a BamHI site (supplemental Table 2). The PCR products were treated with DpnI (New England Biolabs, Ipswich, MA), followed by digestion with XbaI and BamHI in NEB buffer 3 containing bovine serum albumin (New England Biolabs, Ipswich, MA). The purified plasmid was similarly digested. The remaining procedures were the same as described above for pBAD33.1, except that Antarctic phosphatase (New England Biolabs, Ipswich, MA) was used. To avoid heating during chemical transformation, the ligation products were transformed into DH10B (Invitrogen) by electroporation. The desired transformants were selected for chloramphenicol resistance at 30 °C, and the insertions were confirmed using the common primers M13F and M13R2 (supplemental Table 1) (35).

Complementation of the Triple pgp Mutant and Growth at 30 or 42 °C—Growth of YL24/pMAK-A, YL24/pMAK-B, and YL24/pMAK-C (Table 1) at 30 or 42 °C, the permissive and nonpermissive temperatures for the pMAK705-derived hybrid plasmids, was measured in liquid LB medium at A_{600} and compared with the growth of the parental strain W3110. Typically, 30 °C overnight cultures of YL24/pMAK-A, YL24/pMAK-B, or YL24/pMAK-C were diluted to a starting A_{600} of ~0.03 and grown at 30 °C to A_{600} ~0.2. These cultures were then shifted from 30 to 42 °C by a 1:20 dilution into fresh medium, which had been pre-warmed to 42 °C in a shaking water bath. Growth was monitored by measuring the A_{600} every 30 min. The cultures were diluted 1:20 whenever A_{600} reached 0.2, and the A_{600} corrected for the dilution factor was calcu-

lated to construct the cumulative growth curve. This maneuver was necessary because of relatively long lag required to dilute out the covering plasmid and the various Pgp proteins synthesized at 30 °C. Lipid samples were prepared in parallel for LC/ESI-MS/MS analysis from cells growing at 30 °C just before the temperature shift or within an hour of growth cessation at 42 °C.

Lipid Extraction and TLC Analysis—Typically, *E. coli* cells grown on 100 ml of LB broth to A_{600} ~1.0 were collected by centrifugation at 3500 × *g* at 4 °C. The cell pellet was washed with phosphate-buffered saline (PBS) (36), pH 7.4. An acidic Bligh-Dyer extraction (42) was used to recover the phospholipids. The washed cell pellet from the entire culture was suspended in a one-phase Bligh-Dyer mixture, consisting of 16.3 ml of chloroform, methanol, 0.1 M HCl (1:2:0.8 v/v), in which the cell pellet volume was taken into account as part of the aqueous component. The suspension was incubated at room temperature for an hour with intermittent mixing, followed by centrifugation at 3500 × *g* to remove cell debris. The one-phase system was converted into an acidic two-phase Bligh-Dyer mixture, consisting of chloroform, methanol, 0.1 M HCl (2:2:1.8, v/v) by the addition of appropriate volumes of chloroform and 0.1 N hydrochloric acid. After thorough mixing, the phases were separated by centrifugation at 3500 × *g* at room temperature. The lower phase was collected with a glass pipette without disturbing the interface. The bulk solvent was removed by rotary evaporation and remaining traces by evaporation under a stream of nitrogen. The glycerophospholipids were recovered as a yellow-brown oil, which was stored at −20 °C. For different culture volumes, the solvent quantities were adjusted proportionally. In all experiments, the mutants were grown and extracted in parallel with the wild-type strain.

For TLC analysis, lipid samples were dissolved in chloroform/methanol (2:1, v/v) and subjected to sonic irradiation in a bath apparatus for 1 min. Lipid samples (typically 1–5 μg) were loaded onto a TLC or HPTLC Silica Gel 60 plate (EMD, Gibbstown, NJ) and developed in the solvent chloroform, pyridine, 88% formic acid, water (50:50:16:5, v/v). After drying the plate, lipids were visualized by spraying with 10% sulfuric acid in ethanol, followed by charring on a hot plate.

Preparation of Unlabeled PGP—The *pgpApgpC* double mutant YL22 (Table 1) is a practical source of carrier PGP because of its high steady-state PGP levels during exponential growth (Fig. 4*A*). A 1.5-liter culture of YL22 was grown to A_{600} ~1.0. The total lipid was extracted as described above and was fractionated using a 2-ml DEAE-cellulose column (Whatman DE52) prepared in acetate form (37). The entire lipid sample was loaded onto the column in 1 ml of chloroform/methanol/water (2:3:1, v/v) and was eluted stepwise with increasing ammonium acetate; each step consisted of 5 column volumes with either 60, 120, 240, 360, or 480 mM ammonium acetate as the aqueous fraction. The desired fractions were identified by TLC, combined, and converted to a two-phase Bligh-Dyer system by adding appropriate amounts of chloroform and water. The lower phase was concentrated by rotary evaporation. To remove residual contaminating cardiolipin, the sample was further purified on a 2-ml reverse phase column consisting of Bakerbond octadecyl (C_{18}) 40-μm prep LC resin (Mallinckrodt Baker). Solvent A was acetonitrile/water (1:1, v/v), and solvent B was isopropyl alcohol/water (6:1, v/v). The sample was loaded in a mixture of A and B (1: 1, v/v) supplemented with 5 mM tetrabutylammonium phosphate. The PGP was eluted stepwise using 24 ml of A/B (1:1, v/v), 12 ml of A/B (1:2, v/v), and 12 ml of A/B (1:3, v/v). The fractions containing the PGP were combined and diluted 3-fold with chloroform/methanol/water (2:3:1, v/v), which was loaded onto to a 1-ml DEAE column to remove tetrabutylammonium phosphate. The column was washed, and then the PGP was eluted with chloroform, methanol, 480 mM aqueous ammonium acetate (2:3:1, v/v). The purified PGP was recovered by phase portioning as described above and was diluted to make a 2.5 mM stock solution in 50 mM Tris chloride, pH 7.5, containing 0.1% Triton X-100. This material was stored at −20 °C for use in PGP-phosphatase assays. The final yield of PGP was about 0.5 mg from a 1.5-liter culture at A_{600} ~1.

Preparation of Phosphatidyl[U-^{14}C]Glycerol Phosphate—For quantification of PGP-phosphatase activity, phosphatidyl[U-^{14}C]glycerophosphate was employed as the substrate. This material was prepared in one step from [U-^{14}C]glycerol 3-phosphate (PerkinElmer Life Sciences) and CDP-dipalmitoylglycerol (Avanti Polar Lipid, Inc., Alabaster, AL), using *E. coli* PgsA (Fig. 1) as the enzyme (a gift of Dr. W. Dowhan, University of Texas, Houston) (22). The reaction conditions were adapted from a previously described protocol (38). Briefly, the 500-μl reaction mixture contained excess purified PgsA (22), 0.071 mM [U-^{14}C]glycerol 3-phosphate (141 mCi/mmol), 1% Triton X-100, 100 mM Tris chloride, pH 8.0, 0.2 mM CDP-dipalmitoylglycerol, and 100 mM $MgCl_2$. The reaction was initiated by the addition of $MgCl_2$ and incubated overnight at 37 °C. The reaction mixture was then converted into a two-phase Bligh Dyer system consisting of 14.5 ml of chloroform/methanol/water (1:1:0.9, v/v), in which the aqueous phase was generated from 3 ml of 1 M $MgCl_2$, 0.45 ml of 0.1 M HCl, and 0.55 ml of water in addition to the 0.5-ml reaction mixture. The lower phase was collected and dried. The radioactive PGP was resuspended in 200 μl of 100 mM Tris chloride, pH 8.0, and stored at −20 °C; this aqueous PGP dispersion was used in all subsequent PGP phosphatase assays, both for screening and quantification. The yield was 78% based on the input radioactivity.

Screening for PGP-phosphatase Activity and Expression Cloning of pgpC—An *E. coli* genomic DNA library was constructed previously in which 2–6.5-kb fragments of W3110 genomic DNA were inserted into the BamHI site of pACYC184 (25). This plasmid library was transformed into competent YL7 cells (lacking *pgpA* and *pgpB*) by electroporation. A portion of the transformation mixture was spread onto LB agar plates supplemented with chloramphenicol. After incubation at 37 °C overnight, ~400 colonies were obtained on each plate. Single colonies were then picked and inoculated into 200 μl of LB medium containing chloramphenicol prepared in 96-well microtiter plates (28 total). After overnight growth at 37 °C with shaking, 10 μl of each culture was added to 5 μl of 50% glycerol to generate glycerol stocks, which were stored at −80 °C. The cells in the remaining 190 μl of the

overnight cultures were collected by centrifugation at 3500 × *g* at 4 °C, and sets of five pellets were then combined to generate pools of five in ~200 μl of LB medium. The medium was removed by centrifugation, and the pooled pellets were digested with 50 μl of 100 mg/ml lysozyme (Sigma) in 50 mM Tris chloride, pH 8.0, for 30 min at room temperature, followed by freezing at −80 °C for at least 1 h. The digested pools were then thawed at 30 °C for 30 min prior to assaying PGP-phosphatase activity. To initiate the 15-min screening reaction at 22 °C, 5 μl of each pool was mixed with 5 μl of an assay mixture prepared to generate the final concentrations in the assay of 50 mM Tris chloride, pH 7.5, 0.1% Triton X-100, 2 mM $MgCl_2$, 5 mM β-mercaptoethanol, and 1.6 μM phosphatidyl-[U-^{14}C]glycerophosphate (500 cpm/μl). The reactions were terminated by spotting 5-μl samples of each reaction onto the origins of silica TLC plates, which were dried with a cool air stream for 5 min. The plates were developed as described above, dried under a stream of hot air to remove the chromatography solvent, and exposed to a PhosphorImager screen. The radioactive substrates and products for each pool were visualized and quantified with Storm 840 PhosphorImager (GE Healthcare), equipped with ImageQuant software. The percent conversion of substrate to product was determined for each pool. The pools that showed significantly increased PGP-phosphatase activity (~4-fold) relative to the vector controls were identified, and the corresponding individual transformants were re-cultured from the glycerol stocks. The same sample preparation and assay conditions were employed to characterize the individual transformants. Subsequently, the desired plasmids were isolated, and the inserts were sequenced using the primers nACYCfor and nACYCrev (supplemental Table 2). The inserted sequences were aligned with the wild-type *E. coli* genome to reveal novel structural gene(s) encoding PGP-phosphatase(s). Subsequently, the activity was further characterized after transforming the isolated hybrid plasmids into YL7 and repeating the assay procedure.

Quantitative PGP-phosphatase Assays and Characterization of the Activity—To quantify PGP-phosphatase activity, membranes were prepared from 100 ml of LB cultures grown to A_{600} ~1.0. The cells were collected by low speed centrifugation, washed once with phosphate-buffered saline, and resuspended in 2 ml of PBS on ice. The cells were broken by passage through a French pressure cell at 18,000 p.s.i. Large cell debris was removed by centrifugation at 12,000 × *g* for 15 min at 4 °C. The supernatant was transferred to a clean tube and centrifuged at 110,000 × *g* for 1 h at 4 °C to obtain the membrane pellet. After removal of the supernatant, the membranes were homogenized in 0.5 ml of PBS and stored at −80 °C. The protein concentration was determined by the bicinchoninic acid assay using BSA as the protein standard (39). When necessary, the membranes were diluted with PBS to monitor PGP-phosphatase activity in the linear range with respect to time and protein concentration. The PGP-phosphatase assay conditions with isolated membranes were otherwise similar to those described above for the screening assay, except that the concentration of the Tris chloride, pH 7.5, buffer was doubled, and 100 μM nonradioactive carrier PGP was included in the final assay mixture in addition to the phosphatidyl[U-^{14}C]glycerol phosphate at 500 cpm/μl. Specific activity was expressed as nanomoles/min/mg at the indicated assay temperatures. The TLC analysis of product formation was the same as above. The Mg^{2+} dependence of each PGP-phosphatase was assessed by comparing the activity in the presence of 2 mM $MgCl_2$ to no addition or to supplementation with 2 mM EDTA in the assay.

LC/ESI-MS/MS Analysis of E. coli Lipids—Normal phase liquid chromatography was performed on an Agilent 1200 Quaternary LC system equipped with an Ascentis Silica HPLC column, 5 μm, 25 cm × 2.1 mm (Sigma) (40). Mobile phase A consisted of chloroform/methanol/aqueous ammonium hydroxide (800:195:5, v/v); mobile phase B consisted of chloroform/methanol/water/aqueous ammonium hydroxide (600:340:50:5, v/v); mobile phase C consisted of chloroform/methanol/water/aqueous ammonium hydroxide (450:450:95:5, v/v). The elution scheme for the column after loading of the sample was as follows: 100% mobile phase A was held constant for 2 min, followed by a linear increase to 100% mobile phase B over 14 min. The column was then held at 100% mobile phase B for 11 min, followed by a linear change to 100% mobile phase C over 3 min. Finally, the mobile phase was set at 100% mobile phase C for 3 min. The column was returned to 100% mobile phase A over the course of 0.5 min and then held at 100% mobile phase A for 5 min prior to application of the next sample. The LC flow rate was 300 μl/min. The post-column splitter diverted ~10% of the LC effluent into the mass spectrometer, a QSTAR XL quadrupole time-of-flight tandem mass spectrometer (Applied Biosystem, Foster City, CA). Instrumental settings for negative ESI and MS/MS analysis of lipid species were as follows: spray voltage = −4500 V; curtain gas = 20 p.s.i.; ion source gas 1 = 20 p.s.i.; de-clustering potential = −55 V; and focusing potential = −150 V. The MS/MS analysis used nitrogen as the collision gas. Each injection consisted of about 0.1% of the total lipid extracted from a 200-ml *E. coli* culture, typically in 10 μl of chloroform/methanol (2:1, v/v). Data analysis was performed using Analyst QS software (Applied Biosystem, Foster City, CA).

Quantification of PGP Levels Relative to PE from LC/ESI/MS Data—Synthetic standards for the quantification of PGP levels by mass spectrometry are not currently available. Because the absolute quantity of a particular lipid cannot be determined by MS analysis unless an internal standard is also included, the PGP levels in our mutants were expressed as a ratio normalized to the amount of PE present in the same sample. The peak areas of the extracted ion currents of specific PGP species in the chromatograms were integrated using Analyst QS software. The area count numbers were used to estimate the PGP content in each sample. For PE, the most prominent peak seen near *m/z* 688.5 was used as a reference. For PGP, two major doubly charged species found near *m/z* 399.2 and 413.2 and the corresponding singly charged species found near *m/z* 799.5 and 827.5 were used to estimate the area; the total PGP ion current was taken as the sum of these four species. To account for variations in cell density in different samples, the summed areas of the PGP peaks were nor-

TABLE 1
Strains of *E. coli* K12

Strain	Relevant genotypes	Source or Ref.
W3110	Wild type	*E. coli* Genetic Stock Center, Yale
JW0408	BW25113 Δ*pgpA*::Kan^R	27
JW1270	BW25113 Δ*pgpB*::Kan^R	27
YL1	W3110 Δ*pgpA*::Kan^R	This work
YL3	W3110 Δ*pgpB*::Kan^R	This work
YL4	W3110 Δ*pgpB*; derived from YL3	This work
YL7	W3110 Δ*pgpB* Δ*pgpA*::Kan^R; derived from YL4	This work
YL10	W3110 Δ*pgpB* Δ*pgpA*; derived from YL7	This work
WT/pACYC184	W3110 pACYC184	This work
YL7/pACYC184	YL7 pACYC184	This work
JW5408	BW25113 Δ*pgpC*::Kan^R	27
YL20	W3110 Δ*pgpC*::Kan^R	This work
YL21	W3110 Δ*pgpC*; derived from YL20	This work
YL22	W3110 Δ*pgpC* Δ*pgpA*::Kan^R; derived from YL21	This work
YL23	W3110 Δ*pgpC* Δ*pgpB*::Kan^R; derived from YL21	This work
WT/pBAD33.1	W3110 transformed by pPAD33.1	This work
YL7/pBAD33.1	YL7 transformed by pBAD33.1	This work
YL7/pBAD-A	YL7 pBAD-A	This work
YL7/pBAD-B	YL7 pBAD-B	This work
YL7/pBAD-C	YL7 pBAD-C	This work
YL10/pMAK-A	YL10 pMAK-A	This work
YL10/pMAK-B	YL10 pMAK-B	This work
YL10/pMAK-C	YL10 pMAK-C	This work
YL24/pMAK-A	W3110 Δ*pgpB* Δ*pgpA* Δ*pgpC*::Kan^R pMAK-A; derived from YL10/pMAK-A	This work
YL24/pMAK-B	W3110 Δ*pgpB* Δ*pgpA* Δ*pgpC*::Kan^R pMAK-B; derived from YL10/pMAK-B	This work
YL24/pMAK-C	W3110 Δ*pgpB* Δ*pgpA* Δ*pgpC*::Kan^R pMAK-C; derived from YL10/pMAK-C	This work

malized to the endogenous PE level, assuming that the PE content was unaffected when the PG pathway was perturbed. Wild-type PGP levels were normalized to 1. This corresponds to a PGP content of about 0.1% of the total cellular phospholipid based on previous radiochemical labeling studies (16, 23).

RESULTS

Identification of a Gene Encoding a Third PGP-phosphatase in E. coli—Previous studies showed that extracts of a pgpApgpB double mutant contain reduced PGP-phosphatase activity compared with controls when assayed at 42 °C (16, 23). However, significant residual activity is present at 30 °C (23). We constructed a new double deletion mutant lacking *pgpA* and *pgpB* by $P1_{vir}$ transduction of the well characterized mutations of the Keio collection (27) into *E. coli* K12 W3110 to yield mutant YL7 (Table 1). Like previous constructs of this kind, extracts of YL7 had low levels of PGP-phosphatase activity at 42 °C but normal residual activity at 22 °C (see below).

An *E. coli* genomic library harbored in pACYC184 (25) was transformed into YL7, and colonies were selected by growth on LB agar plates containing 25 μg/ml chloramphenicol at 37 °C. Individual transformants were picked and inoculated into microtiter plate wells containing 200 μl of LB medium supplemented with 25 μg/ml chloramphenicol. Following overnight growth at 37 °C, the cultures were pooled into sets of five, lysed with lysozyme, and assayed for activity as described under "Experimental Procedures." After 2750 colonies were screened as 550 pools of five, six pools were identified with increased PGP-phosphatase activity. An example of an active pool is shown in Fig. 2*A*. Under the screening conditions employed, extracts of W3110 and YL7 catalyzed ~12 and 10% conversion of PGP to PG, respectively, in 15 min at 22 °C. Pools with significantly increased phosphatase activity generated 4–5 times more product than the others (Fig. 2*B*).

Each of the five transformants comprising the active pools were grown in separate wells and assayed again in the same manner. Following identification of the plasmids responsible for the high activity extracts, the plasmids were isolated and re-transformed into YL7 to confirm increased PGP-phosphatase activity. Sequencing of these plasmids showed that one contained the chromosomal region corresponding to *pgpA*, whereas the other five carried the *yfhB* locus (26) as their only common gene. However, the inserted DNA fragments were not identical. Sequence analysis revealed that YfhB is a putative membrane protein of unknown function, consisting of 211 amino acid residues and a single predicted membrane-spanning segment (residues 36–54). YfhB is very distantly related to the *E. coli* serine-phosphate phosphatase (SerB), a soluble protein (41). Because no previous functional studies of YfhB have been reported, the *yfhB* gene was renamed *pgpC*.

Overexpression of PGP-phosphatase from pgp Genes Cloned into pBAD33.1—The *pgpA*, *pgpB*, and *pgpC* genes were cloned into pBAD33.1 (Table 2), and the resulting hybrid plasmids were transformed into YL7. Next, YL7/pBAD-A, YL7/pBAD-B, and YL7/pBAD-C, along with their vector controls W3110/pBAD33.1 and YL7/pBAD33.1, were grown to late log phase in LB medium supplemented with chloramphenicol. Expression was induced with 0.2% L-arabinose, which was added to the culture medium at the time of inoculation (A_{600} ~0.03). After A_{600} reached ~1.0, each culture was split into two equal portions. One was used to prepare membranes, and the other was used for lipid extraction. The membranes (0.1 mg/ml) were assayed at 22 °C for PGP-phosphatase activity under the same conditions used for the screening assays (Fig. 3*A*). Extremely high PGP-phosphatase activities were detected in membranes derived from each of the three clones, when compared with the vector controls (Fig. 3*A*).

To confirm that the *pgp* genes are functional *in vivo*, the PGP levels in cells were measured using LC/ESI-MS in the

negative ion mode. The amount of PGP was normalized to the endogenous PE level, as described under "Experimental Procedures," and arbitrarily set to 1.0 in the wild type (Fig. 3*B*). This level corresponds to ~0.1% of the total phospholipid as judged by $^{32}P_i$ labeling studies (16, 23). The *pgpApgpB* double mutant YL7 contained 17 times more PGP than W3110, consistent with previous radiochemical data (Fig. 3*B*) (16, 23). Overexpression of each of the *pgp* genes in the YL7 background lowered the endogenous PGP levels to nearly normal, indicating that all three proteins display PGP phosphate activity in living cells (Fig. 3*B*).

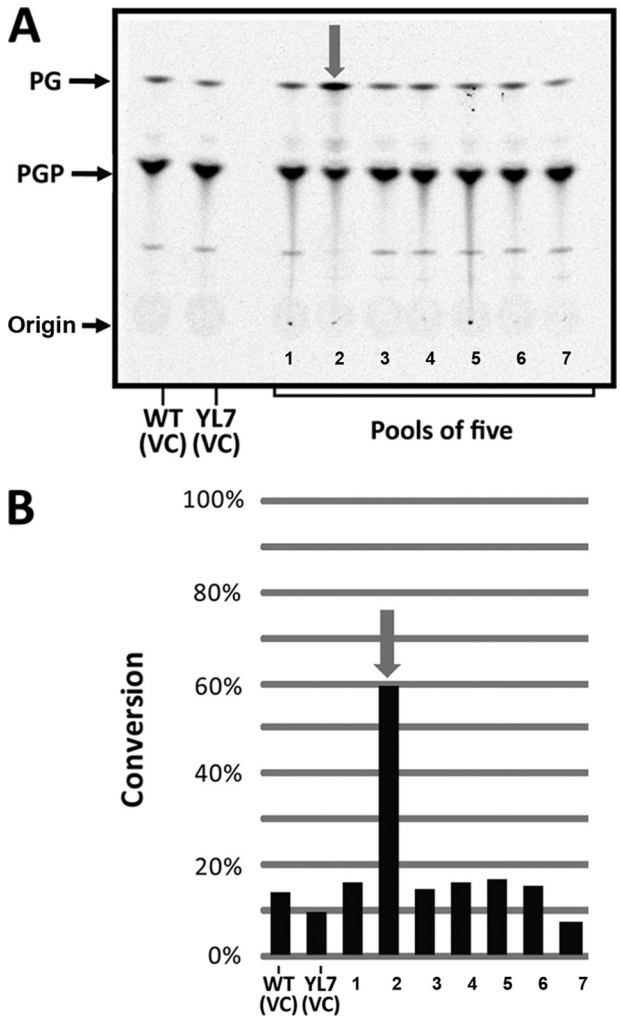

FIGURE 2. **Expression cloning of the *E. coli* PgpC phosphatase.** Pools of cultures of five *E. coli* YL7 colonies, harboring different wild-type *E. coli* DNA fragments on pACYC184, were lysed and assayed for PGP-phosphatase activity at 22 °C using phosphatidyl[U-^{14}C]glycerol phosphate as the substrate. *A*, TLC plate used to assess the extent of PGP dephosphorylation was developed in chloroform, pyridine, 88% formic acid, water (50:50:16:5, v/v). The *1st two lanes on left* are matched extracts of W3110/pACYC184 and YL7/pACYC184, the vector controls. The *2nd lane* of the seven representative pools of five colonies shows a significant increase in PGP-phosphatase activity, as judged by the increased intensity of the PG spot (*gray arrow*). *B*, PhosphorImager data were quantified and expressed as the % dephosphorylation of the PGP substrate during a 15-min assay. *VC*, vector control.

Single and Double Deletion Mutations in the Chromosomal pgp Genes—Three isogenic single mutants with deletions in the *pgpA*, *pgpB*, or *pgpC* genes (designated YL1, YL3, and YL20, respectively) were constructed by $P1_{vir}$ transduction of the wild-type recipient strain *E. coli* W3110 using the kanamycin insertion mutations of the appropriate Keio collection mutants as donors (Table 1). To generate double deletions in the W3110 background, the kanamycin inserts of YL1, YL3, and YL20 were excised by FLP recombination (27, 33), after which another $P1_{vir}$ transduction could be performed to introduce a second *pgp* gene mutation by selection for kanamycin resistance. Three double deletion mutants (different combination of *pgpA*, *pgpB*, and *pgpC*) were successfully generated in this manner (Table 1). The three double mutants were viable on plates at 37 and 42 °C. Liquid cultures of the single or double mutants generally showed normal or slightly slower growth rates compared with W3110. Only YL22 (Δ*pgpC*Δ*pgpA*::Kan^R) had a significantly slower growth rate with a doubling time of ~1 h at 37 °C.

The lipids of the single and double mutants were extracted from late log phase cells using the Bligh-Dyer method (42) and analyzed by TLC, followed by charring (Fig. 4*A*). YL7 (Δ*pgpB*Δ*pgpA*::Kan^R) and YL22 (Δ*pgpC*Δ*pgpA*::Kan^R) showed detectable PGP accumulation by this criterion. Quantification of the PGP levels relative to PE in each strain by LC/ESI-MS confirmed these findings (Fig. 4*B*). Again, YL7 and YL22 contained the most PGP (~43 and ~96 times more than wild type, respectively). The single mutants YL1 (Δ*pgpA*::Kan^R) and YL3 (Δ*pgpB*::Kan^R) showed 7- and 4-fold PGP accumulation, respectively, whereas YL20 (Δ*pgpC*::Kan^R) did not accumulate PGP (Fig. 4*B*). The double mutant YL23 (Δ*pgpC*Δ*pgpB*::Kan^R) showed a 2-fold accumulation of PGP. The amounts of PE, PG, and CL did not vary significantly among the seven strains (Fig. 4*A*). YL22 emerged as a practical source of PGP because of its high level of PGP in log phase cells. The yield of PGP was 0.5 mg from a 1.5-liter culture, harvested at $A_{600} = 1.0$, as described under "Experimental Procedures."

TABLE 2
Plasmids used in this work

Plasmid	Relevant genotype	Source or Ref.
pCP20	*FLP* recombinase expression; Amp^R Cam^R; temperature-sensitive replicon	33
pACYC184	Medium copy vector; Cam^R	54
pBAD33.1	pBAD33 with pET21b ribosomal binding site; medium copy vector; Cam^R	30
pBAD-A	*pgpA* inserted between NdeI and HindIII of pBAD33.1	This work
pBAD-B	*pgpB* inserted between NdeI and HindIII of pBAD33.1	This work
pBAD-C	*pgpC* inserted between NdeI and HindIII of pBAD33.1	This work
pMAK705	Temperature-sensitive replicon; low copy vector; Cam^R	28
pMAK-A	Derived from pBAD-A; pMAK705 harboring *pgpA*	This work
pMAK-B	Derived from pBAD-B;pMAK705 harboring *pgpB*	This work
pMAK-C	Derived from pBAD-C;pMAK705 harboring *pgpC*	This work

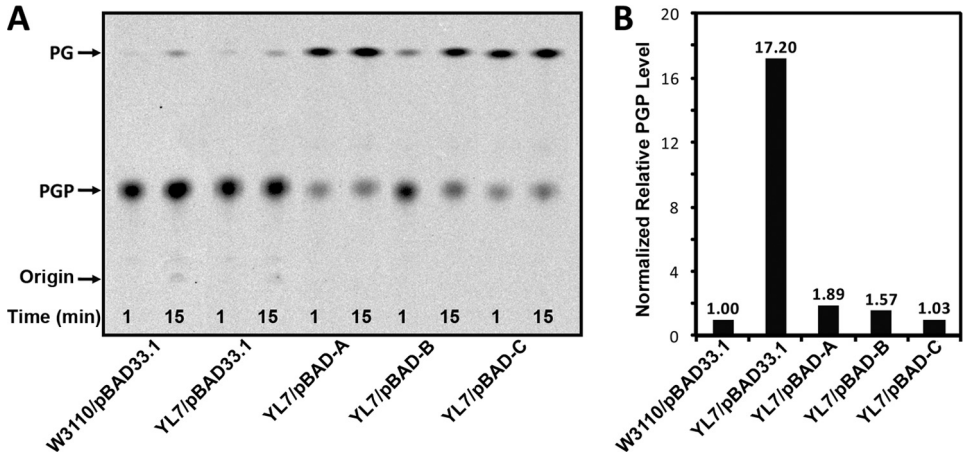

FIGURE 3. **High PGP-phosphatase activity in membranes of cells expressing the *pgp* genes on pBAD33.1.** The two known genes, *pgpA* and *pgpB*, and the newly identified *pgpC* gene were cloned into pBAD33.1, and YL7 host cultures were induced with 0.2% (w/v) L-arabinose. *A,* membranes (0.5 mg/ml) prepared from YL7/pBAD-A, YL7/pBAD-B, and YL7/pBAD-C showed very high levels of phosphatase activity *in vitro* at 22 °C compared with their vector control membranes. PgpA and PgpC membranes were more active than PgpB membranes under these conditions. *B,* lipid profiling by LC/MS confirmed that overexpression of *pgpA*, *pgpB*, or *pgpC* greatly reduces the amount of PGP that accumulates in the parental strain YL7, which lacks both *pgpA* and *pgpB*. The relative levels of PGP were determined by LC/ESI-MS. They were normalized to the endogenous PE in the same sample, which was defined as 1 for the wild-type W3110, corresponding to about 0.1% of the total lipid (16, 23).

PGP-phosphatase Activity and Its Mg^{2+} Dependence in Membranes of the Double Mutants—The PGP-phosphatase activity of the three double mutants was measured at 22 and 42 °C. The membrane samples were prepared from 100-ml cultures that had reached $A_{600} = 1.0$. The membrane concentration was adjusted to 0.5 mg/ml in each assay mixture. As anticipated from previous studies (23), the residual PGP-phosphatase activity in membranes of the *pgpApgpB* double mutant YL7 was temperature-sensitive. As shown in Fig. 5 and Table 3, the specific activity of YL7 membranes was 0.04 nmol/min/mg at 42 °C, although it was 9.94 nmol/min/mg for W3110. When assayed at 22 °C, YL7 membranes were as active as W3110 membranes (4.58 and 3.80 nmol/min/mg, respectively). Membranes of the wild-type W3110, YL22 (Δ*pgpC*Δ*pgpA*::Kan^R), and YL23 (Δ*pgpC*Δ*pgpB*::Kan^R) all displayed higher specific activities at 42 °C compared with 22 °C (Fig. 5). This finding demonstrates that the PgpB and PgpA activities, unlike the PgpC activity, are not temperature-sensitive *in vitro*. YL22 (Δ*pgpC*Δ*pgpA*::Kan^R) activity increased over 7-fold, from 1.68 nmol/min/mg at 22 °C to 12.74 nmol/min/mg at 42 °C. YL23 (Δ*pgpC* Δ*pgpB*::Kan^R) showed relatively low activities at both temperatures as follows: 0.12 nmol/min/mg at 22 °C and 0.88 nmol/min/mg at 42 °C. The specific activities for each strain were calculated from the linear regions of the progress curves within the first 10 min of the time courses (Fig. 5). All three enzymes were assayed under the same standard conditions.

To determine the Mg^{2+} dependence of each PGP-phosphatase, membranes of the three double mutants were assayed at 22 °C for 15 min in the presence of 2 mM $MgCl_2$ or 2 mM EDTA (Fig. 6). Wild-type membranes, which contain all three PGP-phosphatases, are not absolutely dependent upon the addition of Mg^{2+}, because their activity decreased only partially with addition of EDTA. However, PgpA and PgpC are strongly Mg^{2+}-dependent because addition of Mg^{2+} stimulated activity, whereas addition of EDTA abolished it (Fig. 6). Partial activity observed when no Mg^{2+} or no EDTA was added could arise from residual Mg^{2+} carried over from the membrane preparations. Only PgpB is Mg^{2+}-independent, and its activity remains nearly constant under all three conditions (Fig. 6).

Construction of a pgpApgpBpgpC Triple Mutant in the Presence of a Covering Plasmid—Whereas the *pgp* double deletion mutants were viable, a triple deletion mutant of all three *pgp* genes could not be generated by $P1_{vir}$ transduction. However, the triple mutant was easily obtained when a covering plasmid harboring any one of the three *pgp* genes was also present. For this purpose, each of the three *pgp* genes was cloned into the vector pMAK705 (28), which is unable to replicate at 42 °C. These hybrid plasmids, termed pMAK-A, pMAK-B, and pMAK-C (Table 2), were individually transformed at 30 °C into YL10, a *pgpApgpB* double deletion mutant that carries no antibiotic resistance markers of its own (Table 1). Subsequently, triple *pgp* mutants, designated YL24/pMAK-A, YL24/pMAK-B, or YL24/pMAK-C (Table 1), could be generated at 30 °C by $P1_{vir}$ transduction of the *pgpC* kanamycin insertion-deletion mutation from the Keio collection. Triple *pgp* mutants could also be generated in the presence of the covering plasmid pBAD33.1 harboring any one of the three *pgp* genes (data not shown).

Growth Phenotypes of the Triple Mutant Covered by the pMAK-derived Plasmids—The pMAK705 vector contains a temperature-sensitive replicon that results in plasmid loss when the host cells are grown at 42 °C (28). Whereas YL24/pMAK-A, YL24/pMAK-B, and YL24/pMAK-C were viable at 30 °C, no growth was observed when cells were plated on LB agar at 42 °C for 48 h in the absence of antibiotics (Fig. 7*A*). The parental strain W3110 grew well at both temperatures.

To evaluate the growth phenotypes of YL24/pMAK-A, YL24/pMAK-B, and YL24/pMAK-C in greater detail, cells were inoculated into fresh LB broth from an overnight culture grown at 30 °C to yield A_{600} ~0.03. The cells were grown in a shaking water bath at 30 °C until A_{600} reached ~0.2. The cultures were then diluted 20-fold to maintain exponential

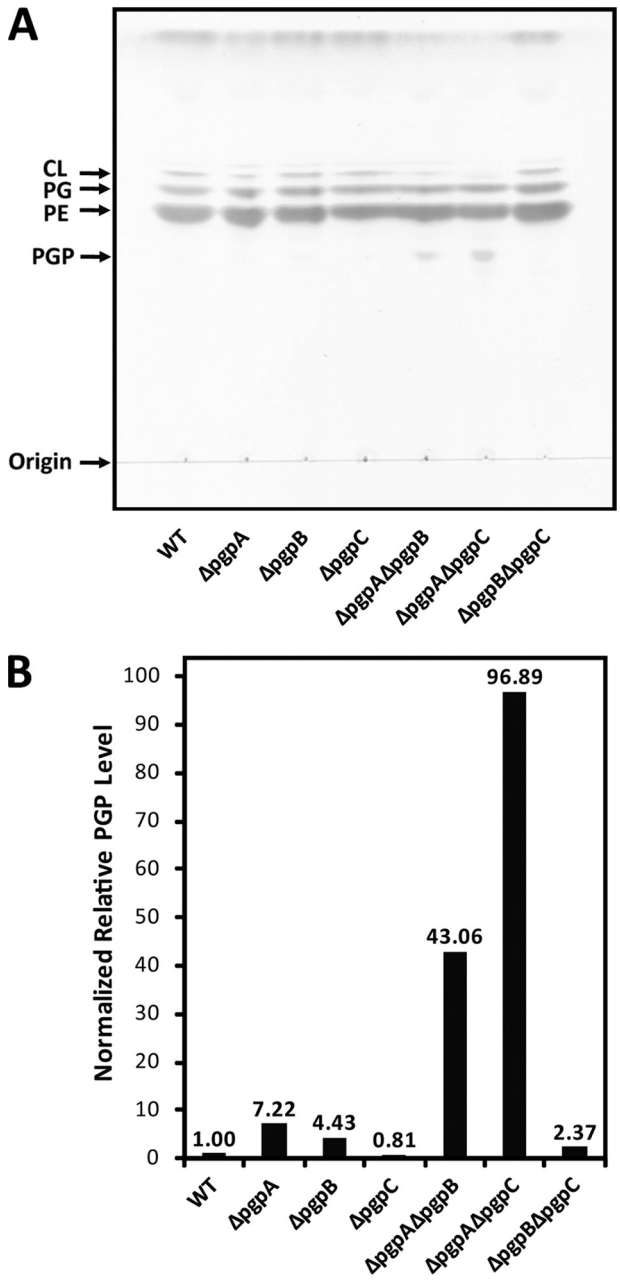

FIGURE 4. **Accumulation of PGP in single and double mutants.** *A*, about 2 μg of total lipids, extracted from the indicated strains using the Bligh-Dyer method, were spotted onto a silica TLC plate, which was developed in chloroform/pyridine/formic acid/water (50:50:16:5, v/v). Lipids were detected by sulfuric acid charring. PE is the most abundant lipid in each strain and serves as the loading control. Visible amounts of a band migrating like PGP accumulate in the *pgpApgpB* and *pgpApgpC* double mutants. *B*, LC/MS confirmed the TLC results. YL22 (Δ*pgpA*Δ*pgpC*) and YL7 (Δ*pgpA*Δ*pgpB*) accumulated the most PGP, whereas the three single mutants and YL23 (Δ*pgpB*Δ*pgpC*) did not accumulate very much PGP. The PGP levels were quantified as in Fig. 3.

growth and simultaneously shifted to a 42 °C water bath with continued shaking. The back-dilution process was repeated whenever the culture reached A_{600} ~0.2, and the cumulative growth yield corrected for dilution was calculated (Fig. 7*B*). All three strains eventually stopped growing after the temperature shift (Fig. 7*B*), although the time of growth cessation varied (~7 h for YL24/pMAK-A, 12 h for YL/pMAK-B, and 3 h for YL24/pMAK-C). The cell densities did not decrease dramatically after growth had stopped.

ESI-MS Analysis of Lipids in the Triple Mutant Covered by pMAK-A, pMAK-B, or pMAK-C—Lipid profiling by LC/MS was performed on the triple mutant covered either by pMAK-A, pMAK-B, or pMAK-C before and after a temperature shift. The 30 °C-grown cells were harvested at $A_{600} = 0.2$. The cells that had been shifted to 42 °C were collected within an hour of growth cessation. The total lipids were subjected to normal phase LC/ESI-MS/MS analysis (40), as described under "Experimental Procedures." All three strains showed massive increases in their PGP levels (eluting between 25.5 and 30 min) and reduced amounts of PG (eluting between 9 and 11.5 min) when shifted from 30 to 42 °C (Fig. 8, *A versus C*, and supplemental Figs. 1 and 2).

Fig. 8 shows the LC/ESI-MS analysis of the lipids present in the triple mutant covered by pMAK-A. The predominant PGP ions in the negative mode are doubly charged (Fig. 8*D*), consistent with the presence of two phosphate groups in PGP (Fig. 1). However, singly charged $[M - H]^-$ ions of PGP are also present at about one-quarter the intensity of the doubly charged ions (data not shown). The peak at *m/z* 399.21 (Fig. 8*D*) is interpreted as the $[M - 2H]^{2-}$ ion of a PGP molecular species bearing one palmitate and one palmitoleate chain, the $[M - 2H]^{2-}$ ion of which is predicted at *m/z* 399.22. The positions of the acyl chains cannot be deduced from the spectrum, but based on other studies, the palmitate group is situated mainly at the 1-position of the *sn*-glycerol 3-phosphate backbone, and the palmitoleate is at the 2-position (supplemental Fig. 4, *inset*) (5).

The ESI-MS/MS analysis of the peak at *m/z* 399.21 supports the proposed PGP structure. However, because extensive fragmentation occurs during collision-induced activation of the doubly charged ion, the MS/MS of the corresponding singly charged $[M - H]^-$ ion of the same PGP molecular species at *m/z* 799.47 was more informative (supplemental Fig. 4). The observed fragment ions at *m/z* 255.25 and 253.23 (supplemental Fig. 4) confirm the presence of palmitate and palmitoleate, respectively. The peaks at *m/z* 645.50 and 232.97 confirm the presence of the polar headgroup of PGP (supplemental Fig. 4). Additional ESI-MS/MS analyses of the doubly charged peaks at *m/z* 385.20, 398.20, 406.22, and 413.22 (Fig. 8*D*) gave rise to the predicted combinations of acyl chain fragment ions (*i.e.* for the above series C14:0/C16:1, C16:1/C16:1, C16:0/C17-cyclopropane, and C16:0/C18:1, respectively), supporting the assignment of these peaks as arising from other molecular species of *E. coli* PGP.

No PGP was detected at 30 °C in the triple mutant covered by pMAK-A (Fig. 8*B*) or pMAK-C (supplemental Fig. 1*B*). The overproduction of the PpgA or PgpC phosphatases in these constructs at 30 °C may lower the steady-state level of PGP below that seen in wild-type cells (Fig. 3*B*). However, some PGP (about 5% of the level observed at 42 °C) is detectable at 30 °C in the triple mutant covered by pMAK-B (supplemental Fig. 2, *B versus D*), suggesting that the overexpressed PpgB phosphatase is not as effective as PgpA or PgpC in dephosphorylating newly synthesized PGP. Previous studies have shown that the active site of PgpB faces the periplasm

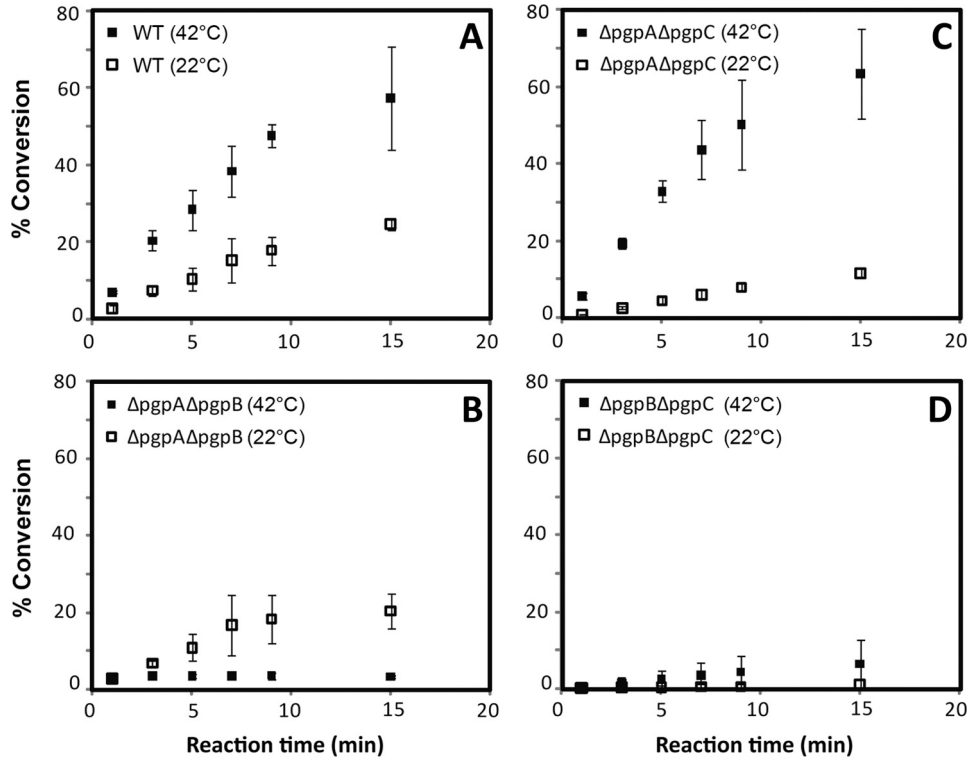

FIGURE 5. **PGP-phosphatase activity in membranes of the double mutants at 22 and 42 °C.** PGP-phosphatase activity was measured using 0.5 mg/ml membranes from the wild type or from each of the double mutants with 100 μM carrier PGP. Accordingly, 10% conversion of substrate to product corresponds to 20 nmol/mg protein, which corresponds to a specific activity of ~9.94 nmol/mg/min for wild-type membranes at 42 °C. *A,* W3110 membranes are more active at 42 than 22 °C. *B,* in contrast, membranes of the mutant lacking both PgpA and PgpB are more active at 22 than 42 °C, consistent with previous reports that residual PGP-phosphatase activity (now ascribed to PpgC) is temperature-sensitive in *pgpApgpB* double mutants (23). *C,* PgpB is more active at 42 than 22 °C. *D,* same is true of PgpA. Surprisingly, PgpA activity in YL23 is relatively low at both temperatures. However, only one standard condition was employed for assaying all three phosphatases. The optimal conditions for each enzyme have not yet been determined. *Error bars* represent the standard deviations of the averages of three determinations.

TABLE 3

PGP-phosphatase-specific activity in membranes of double mutants at different assay temperatures

Strain	Genotype	Active enzyme[a]	22 °C	42 °C
W3110	Wild type	PgpA, PgpB, PgpC	3.80	9.94
YL7	Δ*pgpB* Δ*pgpA*::Kan^R	PgpC	4.58	0.04
YL22	Δ*pgpC* Δ*pgpA*::Kan^R	PgpB	1.68	12.74
YL23	Δ*pgpC* Δ*pgpB*::Kan^R	PgpA	0.12	0.88

[a] Specific activity was calculated in units of nanomoles/min/mg.

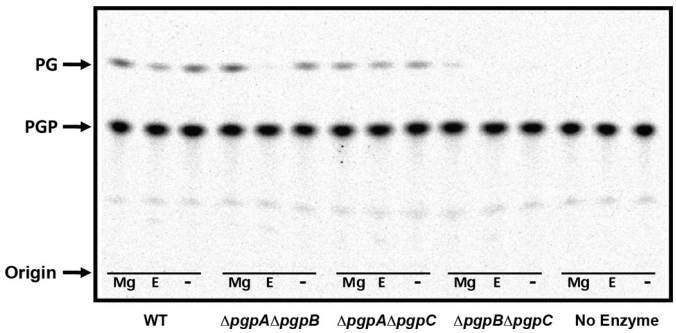

FIGURE 6. **Mg^{2+} dependence of the three *E. coli* PGP-phosphatases.** The three double mutants analyzed in Fig. 5 were used to assess the Mg^{2+} dependence of the three phosphatases, when assayed using 0.5 mg/ml membranes. The indicated conditions are as follows: *Mg*, 2 mM $MgCl_2$ added; *E*, 2 mM EDTA added; and −, no addition. A no enzyme control was included in which PBS replaced the membranes. The wild-type (*WT*) membranes contain all three PGP-phosphatases and are therefore not completely inhibited by EDTA. PgpA and PgpC are both Mg^{2+}-dependent, whereas PgpB is not.

(43), requiring the newly synthesized PGP to flip across the inner membrane prior to dephosphorylation by PgpB. The active sites of PgpA and PgpC probably face the cytoplasmic side of the inner membrane, as suggested by hydropathy analysis (supplemental Fig. 3) and the locations of putative, conserved catalytic residues.

Several other phospholipids accumulated in these constructs after they were shifted to 42 °C (Fig. 8, *A versus C*), including two CL degradation products, tentatively identified as lyso-cardiolipin and bis-lyso-cardiolipin based on their *m/z* values and fragmentation patterns (data not shown), and some methyl-PGP. This compound may arise from PGP as an artifact of Bligh-Dyer extraction under acidic conditions. Although the magnitude of the changes in the PG and CL-related species varied among the three strains (Fig. 8 and supplemental Figs. 1 and 2), the sum of PG, CL, lyso-CL, and bis-lyso-CL remained relatively constant before and after the temperature shift when normalized to the endogenous PE level.

DISCUSSION

E. coli membranes contain several distinct PGP-phosphatases (9, 16, 23). Given that the residual PGP-phosphatase activity in *pgpApgpB* double mutants, like YL7, and related constructs (9, 16, 23) is temperature-sensitive (Fig. 5), we developed a new PGP-phosphatase screening assay that could be used to expression clone additional PGP-phosphatase struc-

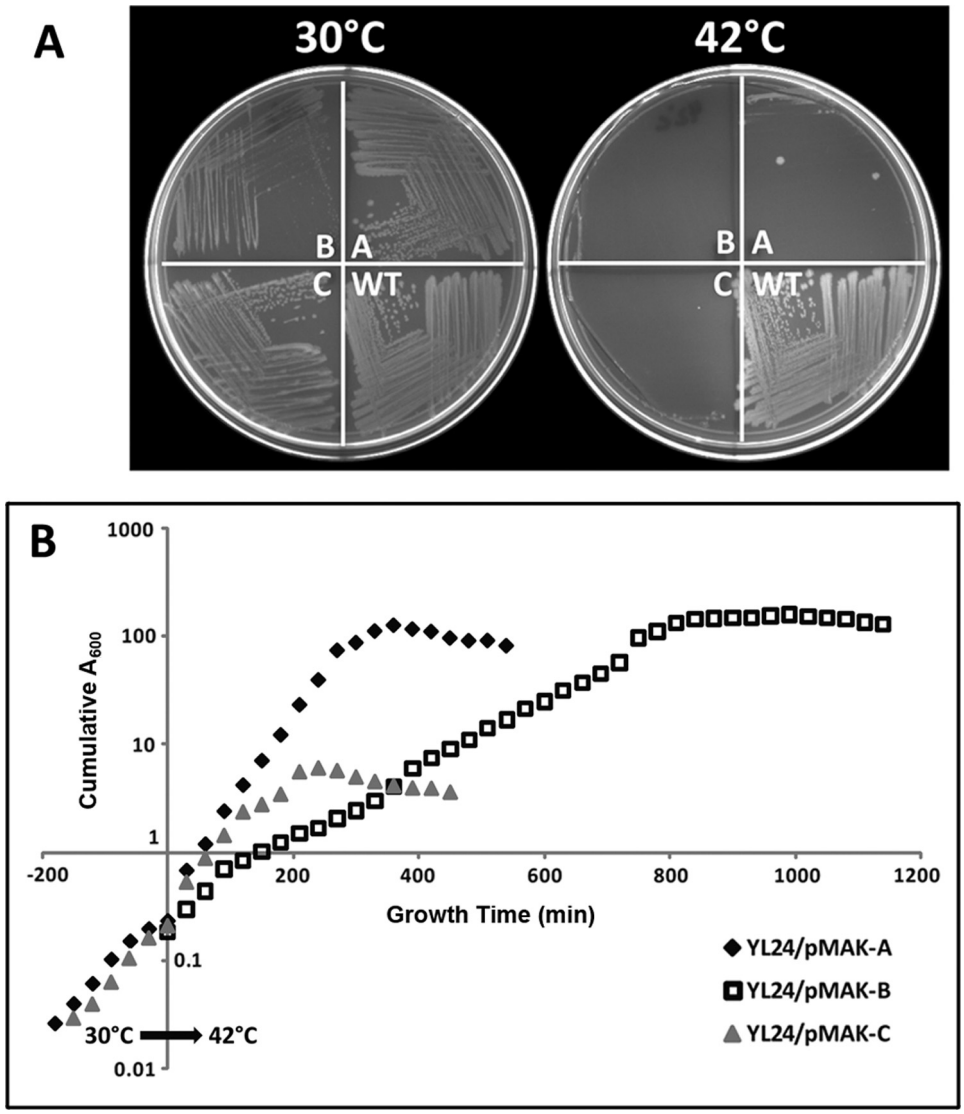

FIGURE 7. **Temperature-sensitive growth of triple mutant YL24 covered by pMAK705 expressing *pgpA*, *pgpB*, or *pgpC*.** *A,* strains YL24/pMAK-A, YL24/pMAK-B, and YL24/pMAK-C (labeled as *A, B,* and *C,* respectively, on the plates) were streaked at 30 or 42 °C. At 42 °C, the complemented strains were unable to form single colonies because of the loss of the covering plasmids. The wild-type W3110 grew well at both 30 and 42 °C. *B,* same complemented strains were grown on LB broth at 30 °C and then shifted to 42 °C at time 0 (*arrow*). YL24/pMAK-B grew more slowly than the others at 30 °C. Its overnight culture had reached A_{600} = 0.3 and thus was used directly without additional pre-shift growth at 30 °C. The *y* axis is the cumulative A_{600} measurement plotted on a log scale, taking into account the back dilutions that were made whenever the cultures reached A_{600} ~0.2. All three strains stopped growing 3–12 h after the temperature shift.

tural genes. This strategy resulted in the identification of YfhB, an uncharacterized membrane protein of unknown function, which is distantly related to the serine-phosphate phosphatase SerB (26). YfhB, renamed PgpC, is a predicted inner membrane protein with a single predicted trans-membrane segment and an active site that likely faces the cytoplasm (supplemental Fig. 3). Like SerB, PgpC is a member of the so-called "haloacid dehalogenase" or "HAD" superfamily of phosphatases (44), which contain several conserved aspartate residues involved in divalent cation binding and covalent catalysis (44). However, in contrast to PgpC, SerB is not a membrane protein.

PgpA and PgpB are also both inner membrane proteins (supplemental Fig. 3), but they share no sequence similarity to each other or to PgpC. PgpB was purified previously, and its substrate selectivity and topography were characterized (43, 45, 46). PgpB contains type 2 phosphatidic acid phosphatase signature residues, does not require divalent cations for catalysis, and faces the periplasm (43). In addition to dephosphorylating PGP, PgpB is one of three enzymes (the others being BacA and YbjG) that dephosphorylate (and thereby recycle) undecaprenyl-diphosphate (46) generated in the periplasm during peptidoglycan polymerization. PgpB also dephosphorylates phosphatidic acid (16), lyso-phosphatidic acid (16), and diacylglycerol-pyrophosphate (45). The substrate selectivity of PgpA has not been fully characterized (16), and the protein has not been purified. However, its active site likely faces the cytoplasm (supplemental Fig. 3), and it belongs to a distinct family of enzymes that feature a pair of divalent cations at their active sites (47). Structural information is available for a distantly related, soluble ortholog of PgpA, but no enzymatic studies were reported for this protein (47).

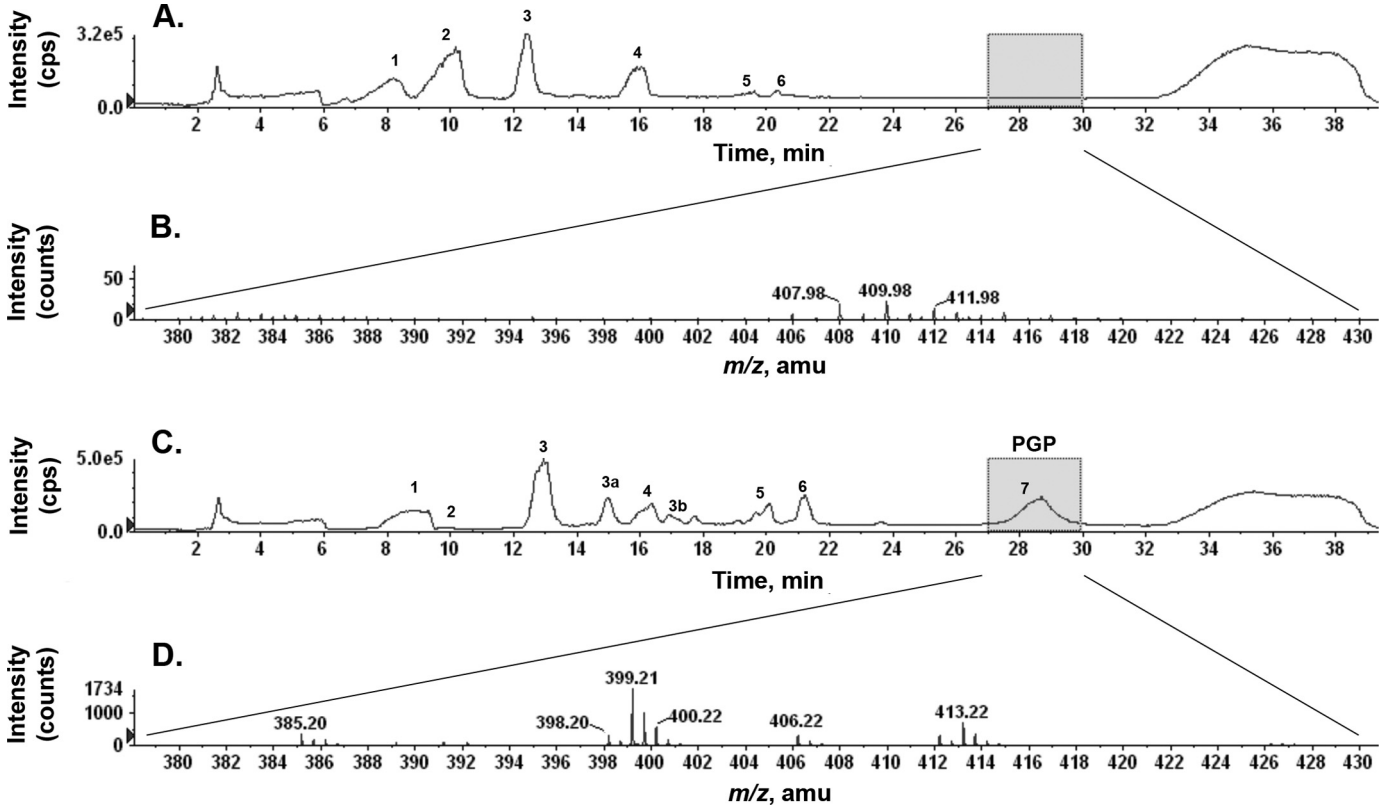

FIGURE 8. **LC/ESI-MS analysis of YL24/pMAK-A lipids from 30 or 42 °C-grown cells.** Total lipids extracted from YL24/pMAK-A were fractionated using normal phase LC and analyzed on line by negative ion ESI-MS (40). *A,* numbers in the total ion chromatogram of the lipids from 30 °C-grown cells indicate the following peaks: *1*, free fatty acids; *2*, PG; *3*, CL; *4*, PE; *5*, lyso-PE; and *6,* phosphatidic acid and undecaprenyl-phosphate. *B,* partial spectrum of lipids from 30 °C-grown cells, eluting between 27 and 30 min in the region expected for PGP. No PGP species were detected in this strain at 30 °C. *C,* numbers in the total ion chromatogram of the lipids from the 42 °C-shifted cells indicate the following peaks: *1,* free fatty acids; *2,* PG; *3,* CL; *3a*, lyso-CL; *3b*, bis-lyso-CL and methyl PGP; *4,* PE; *5,* lyso-PE; *6*, phosphatidic acid and undecaprenyl-phosphate; and *7*, PGP. The lipid composition changed dramatically after the temperature shift with massive accumulation of PGP, loss of PG, and accumulation of lyso-CL, bis-lyso-CL, and methylated PGP. *D,* partial spectrum of the lipids from the 42 °C-shifted cells eluting between 27 and 30 min in the region expected for PGP. Several strong peaks, corresponding to those expected for molecular species of PGP with the fatty acid composition of *E. coli*, were present as doubly charged ions. For instance, the peak at *m/z* 399.21 is attributed to $[M - 2H]^{2-}$ of a PGP species bearing palmitate and palmitoleate. Singly charged ions of the same PGP species were also present at about one-quarter the intensity (not shown). The same lipid analysis is shown for YL24/pMAK-C and YL24/pMAK-B in supplemental Figs. 1 and 2 with similar conclusions.

Construction of a *pgpApgpBpgpC* triple mutant was not possible by $P1_{vir}$ transduction unless a covering plasmid harboring one of the three *pgp* genes was also present, suggesting that no additional PGP-phosphatases exist in *E. coli* grown on nutrient broth. Addition of stabilizing factors, such as 50 mM $MgCl_2$, 0.4 M sucrose, and 2–15% NaCl, as well as lower growth temperatures (22 °C), still did not permit the construction of the triple *pgp* mutant in the absence of a covering plasmid. When the triple mutant YL24 was covered by pMAK705-derived plasmids, which contain a temperature-sensitive replicon, the cells stopped growing after 3–12 h at 42 °C (Fig. 7) and accumulated massive amounts of PGP (Fig. 8 and supplemental Figs. 1 and 2). In parallel, the PG content decreased 5–10-fold. Cardiolipin levels were relatively constant, but lyso- and bis-lyso-cardiolipin accumulated to significant levels. The enzymatic basis for this apparent cardiolipin turnover in *E. coli* is unknown.

The three double mutants were viable. However, the *pgpApgpC* double mutant YL22 grew more slowly than the others, as did the triple mutant YL24 covered by pMAK-B (Fig. 7*B*). PGP transport to the PgpB active site on the outer surface of the inner membrane may be rate-limiting in these constructs. The periplasmic orientation of PgpB (43, 45, 46) may explain the fact that PgpB alone is the least efficient at dephosphorylating PGP *in vivo*, despite its high specific activity *in vitro* (Fig. 5). It may be possible to identify proteins involved in PGP transport from the cytoplasmic to the outer surface of the inner membrane by searching for synthetic lethal mutations in the YL22 background. Because of its relatively high steady-state levels of PGP, YL22 is a convenient source for preparing milligram quantities of this important phospholipid intermediate.

The biological significance of the multiple PGP phosphatases in *E. coli* is uncertain. The distinct membrane topology of PgpB *versus* PgpA and PgpC (supplemental Fig. 3) suggests that there may be extracellular sources of PGP or that it is advantageous to dephosphorylate PGP that prematurely reaches the outer surface of the inner membrane. The membrane-associated members of the PgpA family are found primarily in a subset of Gram-negative bacteria. The PgpB family is more widely distributed and diverse in function. Distant members include the Gram-negative lipid A phosphatases (48–50) and the eucaryotic sphingosine phosphate and lysophosphatidic acid phosphatases, which are located in the plasma membrane and modulate signal transduction (51). PgpC orthologs with a single trans-membrane spanning seg-

ment are present in *E. coli*, *Salmonella typhimurium*, and *Yersinia pestis*. However, PSI-BLAST searching (52) suggests the presence of many additional PgpC-related membrane-bound haloacid dehalogenase family phosphatases in diverse bacteria, such as *Caulobacter crescentus* and *Mycobacterium tuberculosis*. A combination of genetic and biochemical studies will be required to validate the functions of these proteins as true PGP-phosphatases.

Much less is known about eukaryotic PGP-phosphatases. There are no obvious closely related orthologs of PgpA, PgpB, or PgpC in eucaryotic cells. The recently reported yeast PGP-phosphatase Gep4 (53) is required for mitochondrial function and cardiolipin biosynthesis. Gep4 is a member of the larger haloacid dehalogenase-like superfamily, but otherwise it shows no significant similarity to PgpC. Gep4 is nonessential for yeast growth, and considerable residual PG is still synthesized in a Gep4 knock-out (53), demonstrating that at least one additional, novel PGP-phosphatase remains to be discovered in yeast. Interestingly, the *pgpA* gene of *E. coli* can complement the yeast Gep4p mutant (53). Homologs of Gep4 are not present in mammalian cells. Additional PGP-phosphatases must exist in other systems and remain to be identified.

To elucidate the diversity and function of the PGP-phosphatases, the remaining genes encoding enzymes of this kind must still be identified. The regulation, substrate selectivity, chemical mechanisms, and structural biology of these enzymes need to be investigated. Triple mutants, like YL24/pMAK-A, may be very useful for this purpose, because it should be possible to rescue their temperature-sensitive growth phenotype with compatible, temperature-resistant hybrid plasmids expressing heterologous PGP-phosphatases from other sources. Finally, the effects of PGP accumulation on membrane function and the origin of the lyso-cardiolipins remain to be established. A deeper understanding of bacterial membrane assembly and lipid function is certain to emerge.

REFERENCES

1. Kennedy, E. P. (1962) *Harvey Lect. Ser.* **57,** 143–171
2. Raetz, C. R. (1986) *Annu. Rev. Genet.* **20,** 253–295
3. Shibuya, I. (1992) *Prog. Lipid Res.* **31,** 245–299
4. Cronan, J. E. (2003) *Annu. Rev. Microbiol.* **57,** 203–224
5. Zhang, Y. M., and Rock, C. O. (2008) *J. Lipid Res.* **49,** 1867–1874
6. Dowhan, W. (2009) *J. Lipid Res.* **50,** S305–S310
7. Icho, T., Sparrow, C. P., and Raetz, C. R. (1985) *J. Biol. Chem.* **260,** 12078–12083
8. Kanfer, J., and Kennedy, E. P. (1964) *J. Biol. Chem.* **239,** 1720–1726
9. Chang, Y. Y., and Kennedy, E. P. (1967) *J. Lipid Res.* **8,** 456–462
10. Hirschberg, C. B., and Kennedy, E. P. (1972) *Proc. Natl. Acad. Sci. U.S.A.* **69,** 648–651
11. Bos, M. P., Robert, V., and Tommassen, J. (2007) *Annu. Rev. Microbiol.* **61,** 191–214
12. Raetz, C. R., Reynolds, C. M., Trent, M. S., and Bishop, R. E. (2007) *Annu. Rev. Biochem.* **76,** 295–329
13. Raetz, C. R., and Kennedy, E. P. (1972) *J. Biol. Chem.* **247,** 2008–2014
14. Raetz, C. R., and Kennedy, E. P. (1973) *J. Biol. Chem.* **248,** 1098–1105
15. Ganong, B. R., Leonard, J. M., and Raetz, C. R. (1980) *J. Biol. Chem.* **255,** 1623–1629
16. Icho, T., and Raetz, C. R. (1983) *J. Bacteriol.* **153,** 722–730
17. Matsumoto, K. (2001) *Mol. Microbiol.* **39,** 1427–1433
18. Kikuchi, S., Shibuya, I., and Matsumoto, K. (2000) *J. Bacteriol.* **182,** 371–376
19. Shiba, Y., Yokoyama, Y., Aono, Y., Kiuchi, T., Kusaka, J., Matsumoto, K., and Hara, H. (2004) *J. Bacteriol.* **186,** 6526–6535
20. Mileykovskaya, E., Ryan, A. C., Mo, X., Lin, C. C., Khalaf, K. I., Dowhan, W., and Garrett, T. A. (2009) *J. Biol. Chem.* **284,** 2990–3000
21. DeChavigny, A., Heacock, P. N., and Dowhan, W. (1991) *J. Biol. Chem.* **266,** 5323–5332
22. Gopalakrishnan, A. S., Chen, Y. C., Temkin, M., and Dowhan, W. (1986) *J. Biol. Chem.* **261,** 1329–1338
23. Funk, C. R., Zimniak, L., and Dowhan, W. (1992) *J. Bacteriol.* **174,** 205–213
24. Icho, T. (1988) *J. Bacteriol.* **170,** 5117–5124
25. Doerrler, W. T., and Raetz, C. R. (2005) *J. Biol. Chem.* **280,** 27679–27687
26. Blattner, F. R., Plunkett, G., 3rd., Bloch, C. A., Perna, N. T., Burland, V., Riley, M., Collado-Vides, J., Glasner, J. D., Rode, C. K., Mayhew, G. F., Gregor, J., Davis, N. W., Kirkpatrick, H. A., Goeden, M. A., Rose, D. J., Mau, B., and Shao, Y. (1997) *Science* **277,** 1453–1462
27. Baba, T., Ara, T., Hasegawa, M., Takai, Y., Okumura, Y., Baba, M., Datsenko, K. A., Tomita, M., Wanner, B. L., and Mori, H. (2006) *Mol. Syst. Biol.* **2,** 1–11
28. Hamilton, C. M., Aldea, M., Washburn, B. K., Babitzke, P., and Kushner, S. R. (1989) *J. Bacteriol.* **171,** 4617–4622
29. Miller, J. R. (1972) *Experiments in Molecular Genetics*, Cold Spring Harbor Laboratory Press, Cold Spring Harbor, NY
30. Chung, H. S., and Raetz, C. R. (2010) *Biochemistry* **49,** 4126–4137
31. Song, S., Zhang, T., Qi, W., Zhao, W., Xu, B., and Liu, J. (1993) *Chin. J. Biotechnol.* **9,** 197–201
32. Inoue, H., Nojima, H., and Okayama, H. (1990) *Gene* **96,** 23–28
33. Datsenko, K. A., and Wanner, B. L. (2000) *Proc. Natl. Acad. Sci. U.S.A.* **97,** 6640–6645
34. Doublet, B., Douard, G., Targant, H., Meunier, D., Madec, J. Y., and Cloeckaert, A. (2008) *J. Microbiol. Methods* **75,** 359–361
35. Garrett, T. A., Que, N. L., and Raetz, C. R. (1998) *J. Biol. Chem.* **273,** 12457–12465
36. Dulbecco, R., and Vogt, M. (1954) *J. Exp. Med.* **99,** 167–182
37. Raetz, C. R., Purcell, S., Meyer, M. V., Qureshi, N., and Takayama, K. (1985) *J. Biol. Chem.* **260,** 16080–16088
38. Usui, M., Sembongi, H., Matsuzaki, H., Matsumoto, K., and Shibuya, I. (1994) *J. Bacteriol.* **176,** 3389–3392
39. Smith, P. K., Krohn, R. I., Hermanson, G. T., Mallia, A. K., Gartner, F. H., Provenzano, M. D., Fujimoto, E. K., Goeke, N. M., Olson, B. J., and Klenk, D. C. (1985) *Anal. Biochem.* **150,** 76–85
40. Metzger, L. E., 4th, and Raetz, C. R. (2010) *Biochemistry* **49,** 6715–6726
41. Neuwald, A. F., and Stauffer, G. V. (1985) *Nucleic Acids Res.* **13,** 7025–7039
42. Bligh, E. G., and Dyer, W. J. (1959) *Can. J. Biochem. Physiol.* **37,** 911–917
43. Touzé, T., Blanot, D., and Mengin-Lecreulx, D. (2008) *J. Biol. Chem.* **283,** 16573–16583
44. Allen, K. N., and Dunaway-Mariano, D. (2004) *Trends Biochem. Sci.* **29,** 495–503
45. Dillon, D. A., Wu, W. I., Riedel, B., Wissing, J. B., Dowhan, W., and Carman, G. M. (1996) *J. Biol. Chem.* **271,** 30548–30553
46. El Ghachi, M., Derbise, A., Bouhss, A., and Mengin-Lecreulx, D. (2005) *J. Biol. Chem.* **280,** 18689–18695
47. Kumaran, D., Bonanno, J. B., Burley, S. K., and Swaminathan, S. (2006) *Proteins* **64,** 851–862
48. Karbarz, M. J., Kalb, S. R., Cotter, R. J., and Raetz, C. R. (2003) *J. Biol. Chem.* **278,** 39269–39279
49. Wang, X., Karbarz, M. J., McGrath, S. C., Cotter, R. J., and Raetz, C. R. (2004) *J. Biol. Chem.* **279,** 49470–49478
50. Wang, X., McGrath, S. C., Cotter, R. J., and Raetz, C. R. (2006) *J. Biol. Chem.* **281,** 9321–9330
51. Sigal, Y. J., McDermott, M. I., and Morris, A. J. (2005) *Biochem. J.* **387,** 281–293
52. Altschul, S. F., Madden, T. L., Schäffer, A. A., Zhang, J., Zhang, Z., Miller, W., and Lipman, D. J. (1997) *Nucleic Acids Res.* **25,** 3389–3402
53. Osman, C., Haag, M., Wieland, F. T., Brügger, B., and Langer, T. (2010) *EMBO J.* **29,** 1976–1987
54. Chang, A. C., and Cohen, S. N. (1978) *J. Bacteriol.* **134,** 1141–1156